Developmental Cell, Vol. 5, 45–57, July, 2003, Copyright ©2003 by Cell Press

Neuropilin-1 Conveys Semaphorin and VEGF Signaling during Neural and Cardiovascular Development

Chenghua Gu,[1,2] E. Rene Rodriguez,[3] Dorothy V. Reimert,[1,2] Tianzhi Shu,[4] Bernd Fritzsch,[5] Linda J. Richards,[4] Alex L. Kolodkin,[1,*] and David D. Ginty[1,2,*]
[1]Department of Neuroscience
[2]Howard Hughes Medical Institute
[3]Department of Pathology
The Johns Hopkins University School of Medicine
725 North Wolfe Street
Baltimore, Maryland 21205
[4]Department of Anatomy and Neurobiology
School of Medicine
The University of Maryland, Baltimore
Baltimore, Maryland 21201
[5]Department of Biomedical Sciences
Creighton University
Omaha, Nebraska 68178

Summary

Neuropilin-1 (Npn-1) is a receptor that binds multiple ligands from structurally distinct families, including secreted semaphorins (Sema) and vascular endothelial growth factors (VEGF). We generated *npn-1* knockin mice, which express an altered ligand binding site variant of Npn-1, and *npn-1* conditional null mice to establish the cell-type- and ligand specificity of Npn-1 function in the developing cardiovascular and nervous systems. Our results show that VEGF-Npn-1 signaling in endothelial cells is required for angiogenesis. In striking contrast, Sema-Npn-1 signaling is not essential for general vascular development but is required for axonal pathfinding by several populations of neurons in the CNS and PNS. Remarkably, both Sema-Npn-1 signaling and VEGF-Npn-1 signaling are critical for heart development. Therefore, Npn-1 is a multifunctional receptor that mediates the activities of structurally distinct ligands during development of the heart, vasculature, and nervous system.

Introduction

During development, many distinct processes contribute to organ morphogenesis including cell proliferation, migration, differentiation, and neural innervation and vascularization. These developmental events are under the control of numerous cues present in the extracellular environment. One cell surface receptor whose function has been implicated in development of both the cardiovascular and nervous systems is neuropilin-1 (Npn-1), yet the cell-type- and ligand specificity of Npn-1 signaling during development of these interdependent organ systems is not clear.

Npn-1 is a type I transmembrane protein with a small cytoplasmic domain and multiple extracellular domains capable of mediating a variety of protein/protein interactions (Fujisawa et al., 1997). While Npn-1 can mediate heterophilic cell adhesion (Fujisawa et al., 1997; Shimizu et al., 2000), it is also the ligand binding subunit of the semaphorin 3A/collapsin-1 (Sema3A) receptor complex (He and Tessier-Lavigne, 1997; Kolodkin et al., 1997). Semaphorins comprise a large family of proteins first described as regulators of axon pathfinding (Huber et al., 2003). Class 3 semaphorins, including Sema3A, are secreted vertebrate semaphorins that can act as potent axon repellents for specific populations of neurons. These ligands appear to exert their chemorepulsive effects via receptor complexes which include the ligand binding subunit Npn-1, or its close family member Npn-2, and a signal transducing subunit consisting of one of four class A plexin proteins (He et al., 2002). Six class 3 secreted semaphorins have been identified, Sema3A, 3B, 3C, 3D, 3E, and 3F, and each of these ligands can bind with high affinity to either Npn-1, Npn-2, or to both. Moreover, Npn-1 is necessary for Sema3A-mediated chemorepulsion, whereas Npn-2 is necessary for Sema3F-mediated chemorepulsion.

Interestingly, Npn-1 is also expressed in endothelial cells and can bind with high affinity to select isoforms of *v*ascular *e*ndothelial *g*rowth *f*actor (VEGF) (Soker et al., 1998). VEGFs, including $VEGF_{165}$, are critical regulators of vasculogenesis, angiogenesis, and vascular remodeling. Likewise, Npn-2 binds to a distinct but overlapping set of VEGF family ligands (Neufeld et al., 2002). The biological effects of VEGFs are mediated by their signaling receptors, the receptor tyrosine kinases Flt-1 (VEGFR-1), Flk-1/KDR (VEGFR-2), and VEGFR-3 (Ferrara, 2001; Neufeld et al., 1999). Thus, VEGF holoreceptors are likely comprised of VEGFR alone or VEGFR complexes with Npn-1 and/or Npn-2. Indeed, overexpression of Npn-1 in vascular endothelial cells enhances both the affinity labeling of $VEGF_{165}$ to VEGFR-2 and also $VEGF_{165}$-induced cell chemotaxis (Soker et al., 1998).

Despite these in vitro findings, how Npn-1 and Npn-2 function in vivo as requisite coreceptors for VEGF ligands during development remains poorly understood. Analysis of *npn-1* and *npn-2* null mice has, however, provided some insight into neuropilin functions in vivo. *npn-1* null mice die midway through gestation, ~E10.5–E12.5, and exhibit defects in the heart, vasculature, and nervous system (Kawasaki et al., 1999; Kitsukawa et al., 1997). Furthermore, a genetic interaction between VEGF and Npn-1 has been observed in zebrafish (Lee et al., 2002). In contrast to *npn-1* null mice, *npn-2* null mice are viable but exhibit multiple nervous system defects and have a paucity of lymphatic vessels (Chen et al., 2000; Giger et al., 2000; Yuan et al., 2002). *npn-1/npn-2* double mutant null mice die early in gestation, around E8, because of severe vascular anomalies in both the embryo and placenta (Takashima et al., 2002). The various defects in *neuropilin* mutant mice could be due to deficiencies of Sema-Npn signaling, VEGF-Npn signaling, or both. In fact, mouse genetic analyses have revealed that, like VEGFs, two secreted semaphorins,

*Correspondence: kolodkin@jhmi.edu (A.L.K.), dginty@jhmi.edu (D.D.G.)

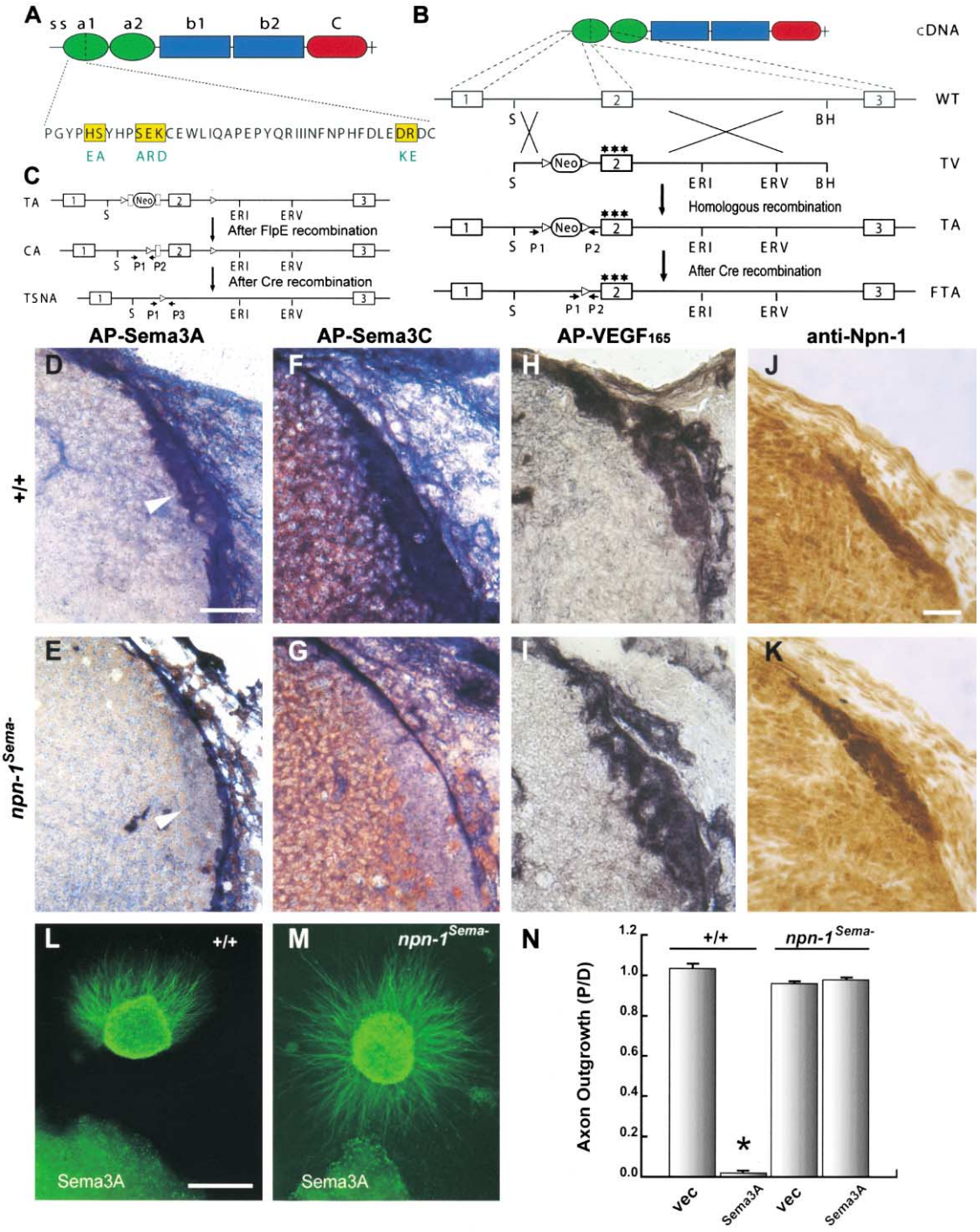

Figure 1. Generation and Characterization of *npn-1*$^{Sema-}$ Mice

(A) Extracellular domain structure of the Npn-1 protein and a 7 amino acid substitution in the N terminus of the Npn-1 a1 CUB domain (Gu et al., 2002).

(B) Gene targeting strategy used to generate *npn-1*$^{Sema-}$ mice. The boxes represent *npn-1* exons 1–3. The targeting vector (TV) contains a mutated exon 2 encoding a 7 amino acid substitution (three stars) and a *pgk-neo* cassette flanked by *loxP* sites (triangles) placed within the intron upstream of exon 2. The *pgk-neo* cassette was excised upon crossing mice with one TA with mice expressing germline Cre-recombinase. The final targeted allele (FTA) contains the mutated *npn-2* exon 2 and one *loxP* site within the upstream intron.

(C) Gene targeting strategy for generation of *npn-1* null and conditional mutant mice. The targeted allele (TA) contains an *FRT* (squares) flanked *neo* cassette and *loxP* sites (triangles) flanking exon 2. After crossing mice harboring the TA with germline FlpE-recombinase mice, the *pgk-neo* cassette was removed and the conditional targeted allele (CA) contained two *loxP* sites flanking exon 2. After crossing with mice carrying Cre-recombinase under the control of the *Tie-2* promoter, exon 2 was excised to generate a tissue-specific *npn-1* null allele (TSNA). *Npn-1* null mice were obtained by crossing mice harboring the CA with mice expressing Cre recombinase in the germline.

(D–I) Alkaline phosphatase (AP)-tagged ligand binding to sections of the DREZ (arrowhead in [D] and [E]) from wild-type littermate controls

Sema3A and Sema3C, control specific aspects of cardiovascular development (Behar et al., 1996; Feiner et al., 2001). Likewise, in addition to their prominent roles as regulators of vascular and heart development, VEGFs may serve as potent trophic factors for motor, sensory, and sympathetic neurons (Oosthuyse et al., 2001; Sondell et al., 1999, 2000). Moreover, both secreted semaphorins and VEGFs are widely expressed within both the nervous system and cardiovascular primordium throughout development. Thus, many secreted semaphorin and VEGF proteins are implicated in both neural and cardiovascular development. *Npn-1* null mice die midway through gestation, very early in the development of the cardiovascular and nervous systems, and therefore how Npn-1 mediates semaphorin and/or VEGF signaling in the heart, vasculature, and nervous system is not known.

To unravel Npn-1's ligand- and cell-type-specific functions and thereby shed light on the regulation of cardiovascular and neuronal development, we sought to selectively disrupt Npn-1 interactions with semaphorins while retaining interactions with VEGFs. Guided by the structure of the bovine Spermadhesin CUB domain (Romero et al., 1997), we identified 7 amino acids located on two adjacent hydrophilic loops of the amino-terminal Npn-1 CUB domain that are critical for binding to the Sema domain of class 3 semaphorins. Substitution of these 7 amino acids completely disrupts Sema-Npn-1 binding but does not affect $VEGF_{165}$-Npn-1 binding or $VEGF_{165}$'s ability to associate with and activate its signaling receptor, VEGFR2 (Gu et al., 2002). Here, we describe a mouse mutant (*npn-1*$^{Sema-}$) that was generated by altering the coding determinants of these 7 amino acids within the *npn-1* locus by homologous recombination in ES cells. The *npn-1*$^{Sema-}$ mouse expresses normal levels of Npn-1 protein, but Sema-Npn-1 signaling is abolished while VEGF-Npn-1 signaling is retained. For complementary analyses, we also used a Cre-loxP strategy to generate a conditional *npn-1* null mouse. Furthermore, we crossed *npn-1*$^{Sema-}$ mice and *npn-2* null mice to generate double mutant mice in which all secreted semaphorin signaling is abolished. Analyses of these mutant mice allow us to determine the ligand- and cell-type specificity of Npn-1 function in vivo. Our findings indicate that Npn-1 coordinates the activities of structurally distinct ligands that control the development of the heart, vasculature, and nervous system.

Results

Generation of *npn-1*$^{Sema-}$ Mice

We first sought to delineate the ligand specificity of Npn-1 function during neural and cardiovascular development. Our recent structure-function analysis revealed that substitution of 7 amino acids located in three regions of the amino-terminal Npn-1 CUB domain completely disrupts Sema-Npn-1 binding but does not affect $VEGF_{165}$-Npn-1 binding or the ability of $VEGF_{165}$ to associate with or activate its signaling receptor, VEGFR2 (Gu et al., 2002). Therefore, we used a gene replacement strategy to generate a knockin mouse, which we call *npn-1*$^{Sema-}$, that expresses only this variant Npn-1 protein (Figure 1). Homozygous *npn-1*$^{Sema-}$ knockin mice express normal levels of Npn-1^{Sema-} protein (Figures 1J and 1K). Moreover, alkaline phosphatase (AP) section binding experiments show that *npn-1*$^{Sema-}$ mice display normal AP-$VEGF_{165}$ binding (Figures 1H and 1I), but little or no AP-Sema3A or AP-Sema3C binding, to endogenous receptors on axons within the dorsal root entry zone (DREZ; Figures 1D–1G). Importantly, neurons from *npn-1*$^{Sema-}$ mice are completely unresponsive to Sema3A. In a three-dimensional collagen matrix, wild-type dorsal root ganglia (DRG) sensory axons were robustly repelled by Sema3A-transfected COS cell aggregates, whereas sensory axons from *npn-1*$^{Sema-}$ mutant mice were not repelled by Sema3A and often grew directly into Sema3A-expressing cell aggregates (Figures 1L–1N).

Interestingly, unlike *npn-1* null mice, which die around E12.5 (Kitsukawa et al., 1997), homozygous *npn-1*$^{Sema-}$ mice survive until birth. This suggests that VEGF-Npn-1 signaling, but not Sema-Npn-1 signaling, is critical for embryonic viability. Approximately 25% of P0 mice from *npn-1*$^{Sema-/+}$ intercrosses are *npn-1*$^{Sema-}$; however, only 60% of these *npn-1*$^{Sema-}$ mice are alive at P7. Seventy percent of P7 survivors are growth retarded, and at least some of these can survive into adulthood. The viability of *npn-1*$^{Sema-}$ mice allowed us to investigate semaphorin-dependent and -independent Npn-1 signaling events during both embryonic and postnatal development. To define the role of Sema-Npn-1 signaling in development of the nervous system, we assessed the integrity of both PNS and CNS projections in *npn-1*$^{Sema-}$ mice and, for comparison, in *npn-1* null embryos when feasible.

Npn-1 and Neural Development

Embryonic Cranial and Spinal Nerves

As observed previously (Kitsukawa et al., 1997), whole-mount neurofilament immunostaining revealed that both cranial and spinal nerves are severely defasciculated and abnormally extended in both E11.5 and E12.5 npn-1 null embryos (Figures 2B and 2F). Abnormal projections of cranial and spinal nerves, including defasciculation and exuberant axon arborizations, were also observed in *npn-1*$^{Sema-}$ mice (Figures 2D and 2H). Interestingly, some of these neural defects appear qualitatively different between *npn-1* null and *npn-1*$^{Sema-}$ mice. For example, distal axons of the ophthalmic nerve in *npn-1* null

(D, F, and H) and *npn-1*$^{Sema-}$ mice (E, G, and I) with AP-Sema3A (D and E), AP-Sema3C (F and G), or AP-VEGF (H and I).
(J–K) Expression of Npn-1 protein in *npn-1*$^{Sema-}$ mice (K) and wild-type littermate control mice (J).
(L–M) DRG sensory neuron axons from wild-type embryos are repelled by Sema3A-expressing COS cells (L) while DRG axons from *npn-1*$^{Sema-}$ embryos are not repelled (M).
(N) Quantitation of repulsion experiments. The repulsive activity is measured by the axon outgrowth ratio P/D, where P is the extent of axon outgrowth on the side proximal to the cell aggregate, and D is the extent of axon outgrowth distal to the cell aggregate. Shown are means ± SEM of 22 (wild-type) and 39 (*npn-1*$^{Sema-}$) explants from three independent experiments ($p < 0.001$, two-way ANOVA). Vec, vector-transfected COS cells; Sema3A, Sema3A-expressing COS cells. Scale bars: (D–I), 50 μm; (J–K), 40 μm; (L–M), 45 μm.

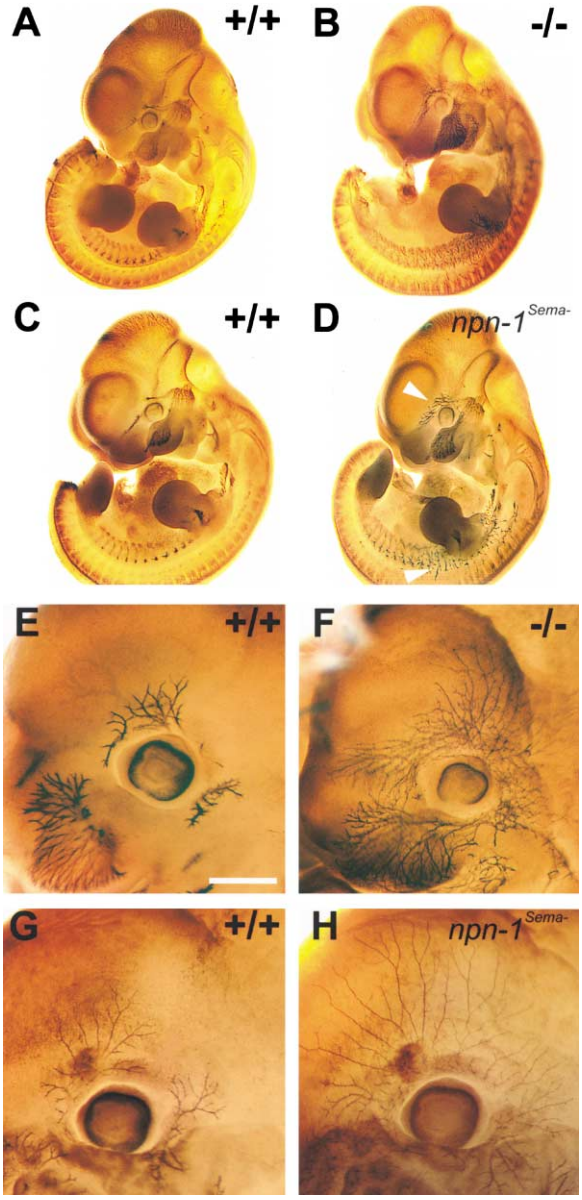

Figure 2. Peripheral Projections of Cranial and Spinal Nerves Are Severely Disorganized in Both *npn-1* Null and *npn-1*$^{Sema-}$ Mice

(A–D) Whole-mount antineurofilament staining of E11.5 *npn-1* null (B), wild-type littermate (A), homozygous *npn-1*$^{Sema-}$ (D), and wild-type littermate (C) embryos. The ophthalmic branch of the trigeminal nerve (upper arrowhead in [D]) and spinal nerves (lower arrowhead in [D]) are disorganized in both *npn-1* null (B) and *npn-1*$^{Sema-}$ mice (D). (E–H) Whole-mount antineurofilament staining of the ophthalmic nerve in E12.5 homozygous *npn-1* null (F), wild-type littermate (E), homozygous *npn-1*$^{Sema-}$ (H), and wild-type littermate (G) embryos. Note the exuberant extension and more regular distribution of ophthalmic nerve branches in *npn-1*$^{Sema-}$ as compared to *npn-1* null ophthalmic projections. Scale bar: (A–D), 0.5 mm; (E–H), 0.2 mm.

mice appear considerably more defasciculated and disorganized than those observed in *npn-1*$^{Sema-}$ mice (Figures 2F and 2H). Axon branches from the ophthalmic nerve extend much further in the *npn-1*$^{Sema-}$ mouse than in either *npn-1* null or wild-type mice, and these branches exhibit a more regular and equally spaced distribution in the region surrounding the developing eye (n = 7). The differences between *npn-1* null and *npn-1*$^{Sema-}$ trigeminal projections may be due to semaphorin-independent Npn-1 functions in these neurons, including axon fasciculation mediated through Npn-1 heterophilic adhesive events (Shimizu et al., 2000; Takagi et al., 1987). Therefore, Sema-Npn-1 signaling is indeed required for cranial and spinal nerve projections, and additional Sema-independent Npn-1 functions may promote fasciculation of some peripheral nerves.

Vestibulocochlear Projections

We next assessed the role of Sema-Npn-1 signaling during development of the vestibulocochlear nerve (nVIII), which conveys sensory information from hair cells of the ear to the brain stem. Lipophilic dye placed into the brainstem shows that afferent fibers of nVIII innervate each of the sensory end organs of the ear by E12.5 (Figure 3A). The E12.5 *npn-1*$^{Sema-}$ mutant mice have additional smaller fiber bundles that extend beyond their normal termination zones within the sensory end organs (Figures 3B and 3C) to form at least three types of defects (four out of four). In most *npn-1*$^{Sema-}$ mice (three out of four), aberrant fibers course between the sensory epithelia of the anterior and horizontal semicircular canal cristae, piercing through the otic capsule to reach the skin above the ear (Figure 3B). In other *npn-1*$^{Sema-}$ mice (three out of four), fibers emanate from the utricle, run anteriorly around the ear, and terminate at or near the posterior canal crista. One *npn-1*$^{Sema-}$ mouse had fibers that formed a loop around the forming cochlea (Figure 3C). Errant projections were not observed in any of the wild-type mice; however, a few errant fibers projecting to the posterior crista were observed in some heterozygous mice (two out of three; data not shown).

These vestibular nerve projection defects persisted in E14.5 (one out of one) and E15.5 (three out of five) *npn-1*$^{Sema-}$ mice but not in either wild-type or heterozygous mice (two out of two). Errant afferent projections extended beyond the anterior and horizontal canal epithelium (Figure 3E), pierced the otocyst wall, and extended toward the auricular branch of the trigeminal nerve (data not shown). Dye injection into auriculotemporal nerve in three separate animals resulted in retrograde labeling of vestibular fibers and neurons in the rostral part of the vestibular ganglion (Figures 3F–3G). Apparently, a subset of afferent fibers of the vestibular nerve project beyond their normal termination fields in the absence of Sema-Npn-1 signaling to innervate areas of the skin normally innervated exclusively by the trigeminal nerve. Nevertheless, these fibers maintain their central projections and terminate in the vestibular nuclei in the brain stem rather than in the nearby trigeminal sensory nuclei (data not shown). Therefore, Sema-Npn-1 signaling is required for guidance of peripheral projections of bipolar neurons of the vestibular ganglion, presumably providing a stop signal near the sensory epithelium.

Sensory Afferent Projections to the Spinal Cord

We next examined the projections of DRG sensory axons into spinal cord gray matter of E14.5 and postnatal day 2 (P2) *npn-1*$^{Sema-}$ mice. Normally, cutaneous afferent

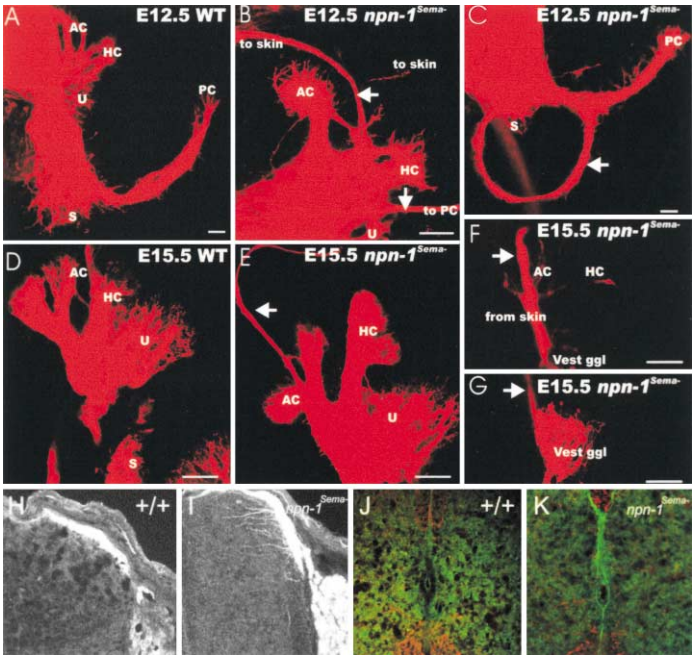

Figure 3. Sema–Npn-1 Signaling Is Required for Sensory Afferent Innervation of the Inner Ear and Spinal Cord

(A–C) In E12.5 *npn-1*$^{Sema-}$ mice, vestibular nerve fibers extend beyond the anterior and horizontal cristae (AC, HC) and reach the skin above the ear ([B], top arrow). In addition, fiber bundles extend from the utricle (U) to the posterior crista (PC) where they may leave the ear through the round window ([B], bottom arrow; data not shown). In some animals, vestibular fibers are observed projecting around the forming cochlea without innervating any target ([C], arrow).

(D–G) E15.5 *npn-1*$^{Sema-}$ mutants form inner ear afferent fibers to the skin. These fibers extend beyond the anterior cristae (E), pass through the otic capsule, and run together with the auriculotemporal nerve to the skin anterior to the auricle (arrow). Injection of dye into this area of the skin labels nVIII fibers that pass through the lateral otic wall (F) and pass underneath the canal cristae where some fibers branch and provide afferents to those epithelia (arrow). These fibers come from vestibular ganglion neurons (G) which project centrally into vestibular nuclei (data not shown).

(H–K) Abnormal central projections of spinal sensory afferents. TrkA immunohistochemistry of E14 (H and I) and P2 (J and K) lumbar spinal cord in *npn-1*$^{Sema-}$ (I and K) and wild-type littermates (H and J), examined by confocal microscopy. Dorsal spinal cord is at the top. Scale bars: (A–G), 100 μm; (H–K), scale bar in (G) is equal to 200 μm in (H)–(K).

axons project to the DREZ and then stall during a "waiting period," which in the mouse extends from ~E11 until ~E15, before innervating the spinal cord. As shown in Figure 3H, TrkA-positive fibers in wild-type embryos are restricted to the DREZ at E14.5 (n = 3). In contrast, many TrkA-positive fibers in *npn-1*$^{Sema-}$ mice have already entered the gray matter at E14.5, and a subset of these errant projections extends into the most ventral regions of the spinal cord (Figure 3I and data not shown; n = 3). At a later time, P2, TrkA-positive fibers in wild-type mice have invaded the spinal cord and are completely restricted to their target fields within the dorsal laminae (Figure 3J, n = 7). In contrast, in *npn-1*$^{Sema-}$ mice, some axons were observed outside of their normal termination zones, traveling along the midline and into the medial-ventral spinal cord (Figure 3K, n = 7). Similar aberrant projections were reported in *sema3A* null mice (Behar et al., 1996). Thus, Sema3A signaling through Npn-1 is indeed required for guiding the central projections of a subset of TrkA-positive axons of cutaneous sensory neurons during development.

Corpus Callosum

Other later developing CNS fiber tracts were also disrupted in *npn-1*$^{Sema-}$ mice including axons of the corpus callosum, which project to the contralateral cortical hemisphere. This fiber tract normally binds avidly to the AP-Sema3A fusion protein (Figure 4I). DiI labeling experiments revealed callosal defects in all E17.5 *npn-1*$^{Sema-}$ embryos examined (Figures 4B, 4C, and 4E–4H, n = 10). Corpus callosum phenotypes varied from mild, in which some callosal axons deviated from the main bundle into the glial wedge and septum but most crossed the midline (Figures 4B and 4E), to more severe phenotypes where the main callosal bundle was highly defasciculated and few, if any, callosal axons crossed the midline (Figures 4C and 4F). In the most extreme cases we observed complete agenesis of the corpus callosum, resulting in the formation of Probst bundles (Figures 4G and H). Callosal defects were not observed in any wild-type or heterozygote littermate controls (n = 10; Figures 4A and 4D).

Entorhinohippocampal Projections

To determine whether Sema-Npn-1 signaling is required for the generation of layer-specific connections in the hippocampus, we next analyzed the development of entorhinohippocampal connections in the *npn-1*$^{Sema-}$ mice. At E18–P2, entorhinal fibers terminate in the stratum lacunosum-moleculare whereas commissural/associational fibers terminate in the stratum radiatum and stratum oriens (Super and Soriano, 1994). For these experiments, DiI was injected into the entorhinal cortex of P2 *npn-1*$^{Sema-}$ mice and wild-type littermate controls to visualize entorhinohippocampal projections. As in previous studies, entorhinohippocampal fibers were restricted in wild-type mice to the ipsilateral stratum lacunosum-moleculare, with no labeled axons present in either the stratum radiatum or stratum oriens (Figure 4J, n = 7). In contrast, in *npn-1*$^{Sema-}$ mice, entorhinohippocampal axons were no longer restricted in the stratum lacunosum-moleculare of the ipsilateral hippocampus. Many fibers had innervated ectopic layers, mostly the stratum radiatum of the CA1 field (Figure 4K, n = 9). An entorhinohippocampal projection defect was also observed in *sema3A* null mice (Pozas et al., 2001), but that phenotype appeared much less severe since most fibers were observed to correctly innervate the stratum lacunosum-moleculare and only a few fibers were found to innervate ectopic hippocampal layers such as the

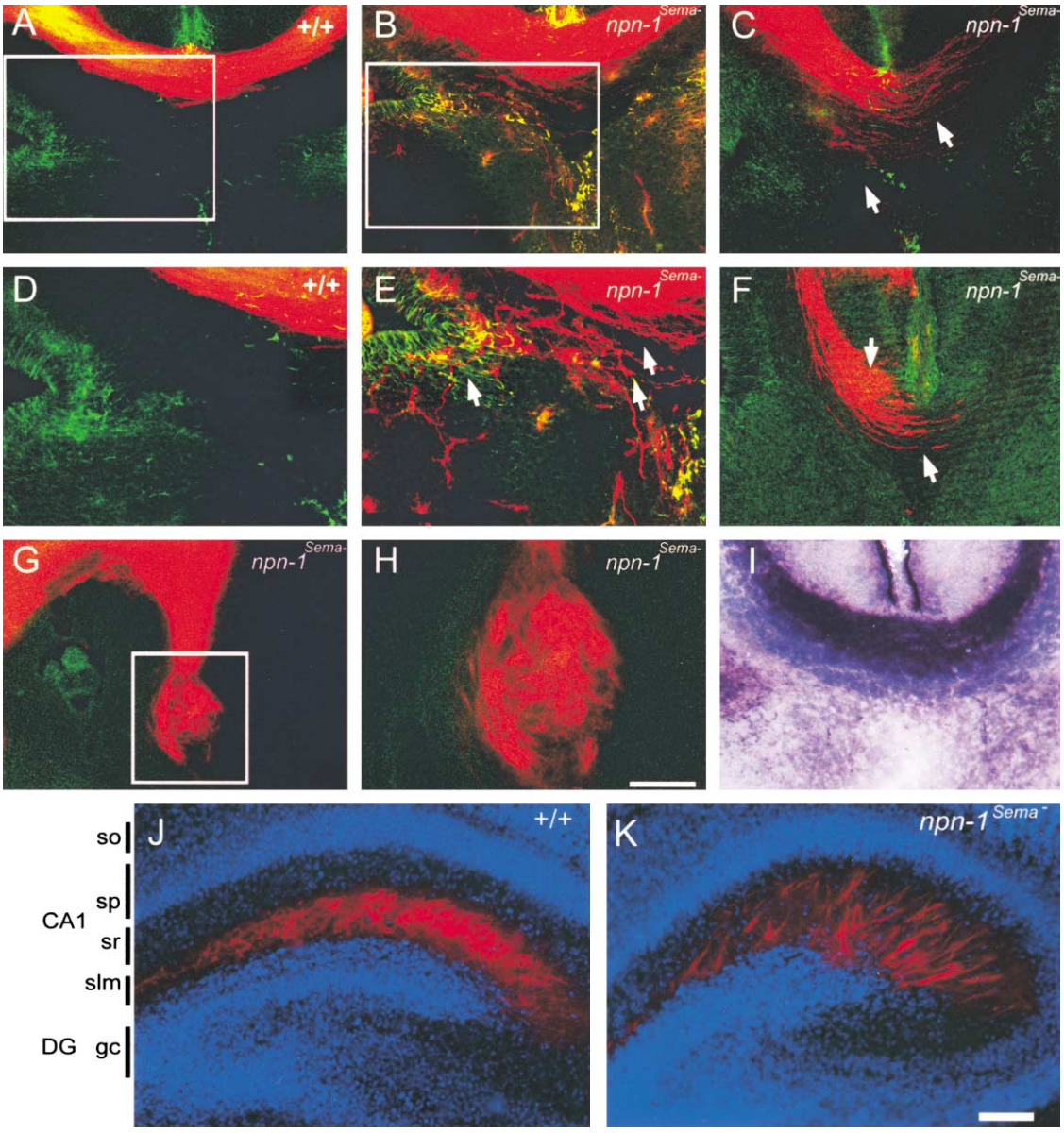

Figure 4. Axonal Projection Defects in the Corpus Callosum and Hippocampus in *npn-1*$^{Sema-}$ Mice

(A–H) DiI labeling at E17.5 was used to investigate development of the corpus callosum in wild-type (A and D) and *npn-1*$^{Sema-}$ mice (B, C, and E–H). The corpus callosum developed normally in all wild-type littermate embryos analyzed (n = 10), whereas in all *npn-1*$^{Sema-}$ embryos examined (n = 10), callosal axons (red) displayed varying degrees of defasciculation from more mild phenotypes (arrows in [E]) to more severe phenotypes (arrows in [C] and [F]). In the most extreme cases, callosal axons formed Probst bundles (G and H). Sections were double labeled with GFAP immunohistochemistry to label midline glial structures (A–H). In some cases, axons grew through the glial wedge (green labeling in [E]) and into the septum.

(I) AP-Sema3A section binding reveals a high level of Sema3A binding to axons of the E17.5 corpus callosum in wild-type mice. (D), (E), and (H) are high-magnification views of the boxed regions in (A), (B), and (G), respectively.

(J–K) Sema-Npn-1 signaling is crucial for layer-specific targeting of entorhinohippocampal projections. Coronal sections of brains of P2 wild-type (J) and *npn-1*$^{Sema-}$ littermate mice (K) showing DiI-labeled (red) entorhinohippocampal axons. The sections were counterstained with bisbenzimide (blue) to reveal the hippocampal architecture. In wild-type mice, entorhinal fibers (red) are restricted to the stratum lacunosum moleculare (slm) (J). In contrast, entorhinal fibers of *npn-1*$^{Sema-}$ mice are found in the slm layer and also ectopic layers such as the stratum radiatum (sr) of the CA1 field (K). DG, dentate gyrus; slm, stratum lacunosum moleculare; sp, stratum pyramidale; sr, statum radiatum. Scale bars: (A–C, F, and I), 150 μm; (G), 200 μm; (H), 60 μm; (J and K), 100 μm.

stratum radiatum and the hilus (Pozas et al., 2001). Therefore, we conclude that Sema3A, and probably additional secreted semaphorins in the hippocampus, act through Npn-1 to restrict axonal projections of entorhinohippocampal neurons to their specific targets within the stratum lacunosum-moleculare.

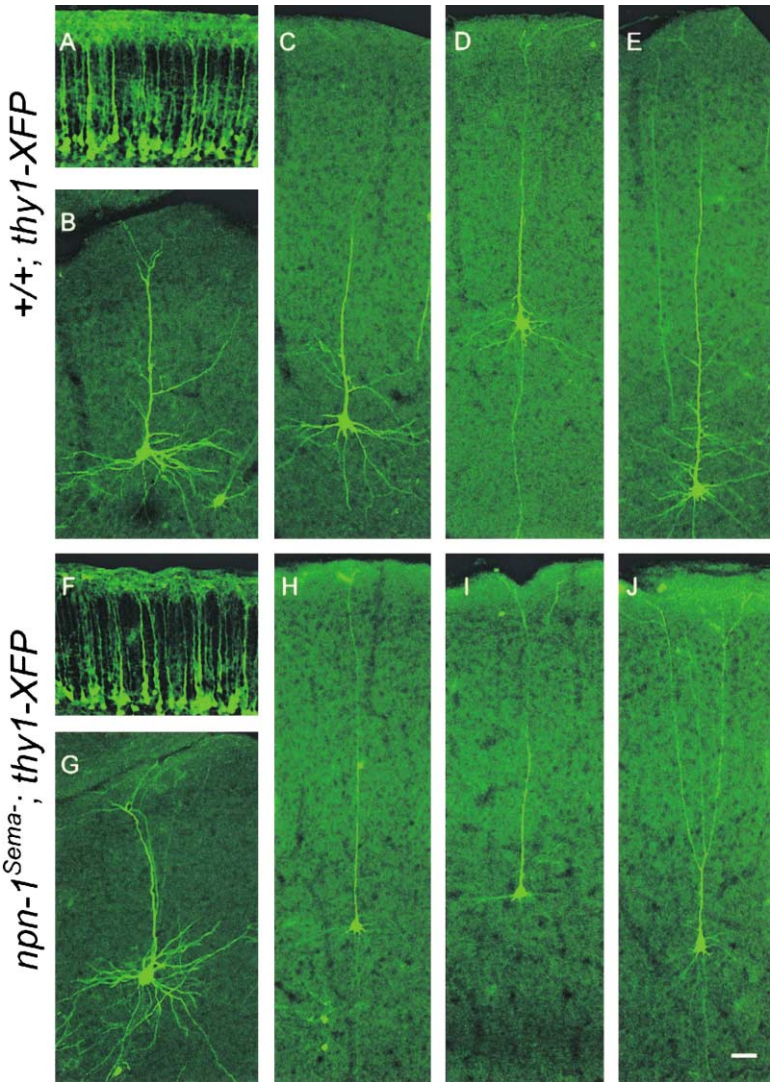

Figure 5. Sema-Npn-1 Signaling Is Required for Growth of Basal Dendrites, but Not for Apical Dendrite Orientation

(A and F) Orientation of apical dendrites of layer 5 pyramidal neurons from neocortex of P2 mutant (*npn-1^{Sema-};thy1-YFP*) (F) and control littermates (+/+;*thy1-YFP*) (A).

(B and G) Similar dendritic morphologies of cingulate cortical neurons from P14 mutant (*npn-1^{Sema-};thy1-GFP-m)* (G) and control littermates (+/+;*thy1-GFP-m*) (B).

(C–E and H–J) Dendritic morphologies of individual GFP-positive pyramidal neurons from P14 mutant (*npn-1^{Sema-};thy1-GFP-m*) (H–J) and control littermates (+/+;*thy1-GFP-m*) (C–E). While apical dendrite and axon orientation appears similar in mutants (H–J) and littermate controls (C–E), basal dendrites are less elaborate in mutants (H–J) compared to controls (C–E). Scale bar: 50 μm.

Cortical Neuron Dendrites

In addition to their roles as axonal chemorepellents, secreted semaphorins have also been implicated in dendrite formation (Behar et al., 1996; Polleux et al., 1998, 2000). Therefore, we next assessed the integrity of both apical and basal dendrites of layer 5 pyramidal neurons of *npn-1^{Sema-}* mice. Since many *npn-1^{Sema-}* mice are viable, our analysis was carried out with P2 (n = 4), P6 (n = 2), and P14 (n = 3) brains, times at which dendrites of layer 5 pyramidal neurons are elaborated. To examine cortical neuron morphology, we crossed *npn-1^{Sema-}* mice with mice that express YFP in all layer 5 neurons (*npn-1^{Sema-};thy1-YFP* mice, Figures 5A and 5F) or in mice expressing GFP in a small subset of neurons (*npn-1^{Sema-};thy1-GFP-m* mice, Figures 5B–5E and 5G–5J) (Feng et al., 2000). Although Sema3A can serve as an attractant for apical dendrites and a repellent for axons of cortical neurons in vitro (Polleux et al., 1998, 2000), we did not observe apical dendrite or axon orientation defects in cortical neurons of either the *npn-1^{Sema-};thy1-YFP* mice (Figure 5F) or the *npn-1^{Sema-};thy1-GFP-m* mice (Figures 5G–5J, and data not shown). We did, however, observe that the basal dendrites of layer 5 cortical neurons within the neocortex (compare Figures 5C–5E and 5H–5J), but not neurons in the cingulate cortex (compare Figures 5B and 5G), of *npn-1^{Sema-};thy1-GFP-m* mice were markedly diminished in both length and complexity. Thus, Sema–Npn-1 signaling contributes to basal, but not apical, cortical neuron dendrite development.

Npn-1 and Development of the Cardiovascular System

While our results support a model in which Sema-Npn-1 signaling is necessary for the establishment of PNS and CNS projections during both early and late embryonic development, the ligand dependence of Npn-1 signaling for cardiovascular system development is more complex. *npn-1* is expressed in multiple cell types that contribute to development of the cardiovascular system including cardiac neural crest cells (Brown et al., 2001; Feiner et al., 2001) and endothelial cells (Soker et al., 1998). Moreover, mice with null mutations in *npn-1*, or in the genes encoding Npn-1 ligands VEGF-A, VEGF-B, PLGF-2, Sema3A, and Sema3C, exhibit heart and/or

vasculature defects (Behar et al., 1996; Brown et al., 2001; Feiner et al., 2001; Kawasaki et al., 1999; Neufeld et al., 1999; Takashima et al., 2002). Thus, to understand how VEGF-Npn-1 signaling and Sema-Npn-1 signaling contribute in vivo to cardiovascular development, we first determined whether Npn-1 is required in endothelial cells for vasculature development.

Npn-1 Signaling and Angiogenesis

Endothelial cell-specific *npn-1* null mice were generated by crossing homozygous "floxed" *npn-1* conditional mice (Figure 1C) with *Tie-2-Cre* transgenic mice (Kisanuki et al., 2001), which express Cre recombinase only in endothelial cells (*C/C;Cre* mice). For some analyses, we employed compound heterozygous mice (one floxed *npn-1* allele, one null *npn-1* allele, and one *Tie-2-Cre* transgenic allele; called *C/−;Cre* mice), which allowed for more efficient Cre-mediated removal of Npn-1. We first examined vasculature integrity in *C/−;Cre* and control littermate mice by whole-mount PECAM immunostaining and isolectin staining. Whole-mount PECAM staining revealed dramatic systemic vascular deficiencies in E12.5 *C/−;Cre* mice which probably account for the mid-to-late embryonic lethality of these mice. For example, the abdominal wall contains only distended vessels and lacks the medium and small-diameter branched vessels readily observed in littermate controls (Figures 6A–6D; n = 4). In addition, isolectin staining of horizontal brain sections from E13.5 *C/−;Cre* mice revealed dramatic defects in the vasculature of the developing brain. While vessels are evenly distributed and normally branched in the developing diencephalon and telencephalon of control embryos (Figures 6G and 6I), vessels in brains from *C/−;Cre* littermates are large, dramatically underdeveloped, and not branched (Figures 6H and 6J, and data not shown). Interestingly, none of these vascular defects were observed in *npn-1*$^{Sema-}$ embryos (Figures 6E, 6F, 6K, and 6L; n = 4). These results show that VEGF-Npn-1 signaling, and not Sema-Npn-1 signaling, within endothelial cells is essential for general development of the vasculature.

Npn-1 Signaling in Heart Development

We next examined the cell-type- and ligand dependence of Npn-1 signaling for development of the heart. For this analysis we used *C/C;Cre* mice, which were found to die perinataly (25 out of 25 animals). These mice exhibit multiple cardiac defects, including persistent truncus arteriosus (Figure 7D; Table 1; 17 out of 17 mice), which results from a failure of septation of the cardiac outflow tract. Thus, *C/C;Cre* mice share common pulmonary artery and aortic roots. Some *C/C;Cre* mutant mice also exhibited misplacement (anomalous origin) of the coronary arteries (Figure 7C and arrow in Figure 7D; Table 1, four out of ten mice) and ventricular septal defects (three out of eight mice, data not shown). Truncus arteriosus was also observed in experiments using *C/−;Cre* embryos (four out of four mice; data not shown). In contrast, truncus arteriosus was not observed in *npn-1*$^{Sema-}$ mice (Figure 7F; Table 1). Thus, Sema-independent Npn-1 signaling in endothelial cells is essential for septation of the cardiac outflow tract and heart development.

While the precise mechanism of outflow tract septation remains to be described, cardiac neural crest cells have been implicated in this process (Creazzo et al., 1999). Interestingly, a previous report showed that one of the secreted semaphorins, Sema3C, is required for septation of the outflow tract, possibly because it guides the migration of cardiac neural crest cells into the proximal outflow tract during heart development (Feiner et al., 2001). While the nature of the Sema3C receptor in vivo is not known, this secreted semaphorin binds with high affinity to both Npn-1 and its close relative Npn-2, and a Npn-1/Npn-2 heterodimer may serve as a Sema3C receptor in sympathetic neurons (Chen et al., 1997, 1998; Takahashi et al., 1998). Since impaired VEGF and/or Sema3C signaling may result in the septation defects observed in *C/C;Cre* mice, we next examined the cardiac outflow tracts in *npn-1*$^{Sema-}$ mice, *npn-2* null mice (Giger et al., 2000), and in *npn-1*$^{Sema-}$;*npn-2*$^{-/-}$ double mutant mice to distinguish between these possibilities. Both *npn-1*$^{Sema-}$ mice and *npn-2* null mice have normal cardiac outflow tracts and great vessels (11 out of 11 mice and 8 out of 8 mice, respectively; Figures 7E and 7F; Table 1). Interestingly, 66% of *npn-1*$^{Sema-}$;*npn-2*$^{-/-}$ double mutant mice displayed a persistent truncus arteriosus (six out of nine; Figures 7H and 7J; Table 1). Some *npn-1*$^{Sema-}$;*npn-2*$^{-/-}$ double mutant mice also exhibited ventricular septal defects (Figure 7K). Since in certain genetic backgrounds a similar outflow tract phenotype was observed in *sema3C* null mice, these results taken together suggest that the Sema3C receptor is either Npn-1 or Npn-2 (either receptor alone being sufficient). Thus, at least two distinct ligands, Sema3C and a VEGF family member, each act through Npn-1 to coordinate outflow tract septation. Finally, nearly all of the *npn-1*$^{Sema-}$ mice (10 out of 11) and *npn-1*$^{Sema-}$;*npn-2*$^{-/-}$double mutant mice (8 out of 9) exhibited bilateral atrial enlargement (Figure 7; Table 1), a defect also noted in the *sema3A* null mice (Behar et al., 1996). It is interesting that we also observed atrial enlargement in *C/−;Cre* mice, raising the intriguing possibility that Sema3A-Npn-1 signaling in endothelial cells contributes to atrial development. These observations indicate that Npn-1 serves as a receptor for both secreted semaphorins and VEGFs to coordinate cardiac development.

Discussion

Our results show that Npn-1 is a receptor for members of structurally and functionally distinct ligand families in vivo. In the nervous system, Npn-1 functions as a receptor for secreted semaphorins, promoting fasciculation and proper targeting of several populations of PNS and CNS projections. Because of the extended viability of *npn-1*$^{Sema-}$ mice compared to *npn-1* null mice, we have uncovered several neural functions of Sema-Npn-1 signaling. Remarkably, we have so far observed no defects in the vasculature of either *npn-1*$^{Sema-}$ (Figure 6) or *npn-1*$^{Sema-}$;*npn-2*$^{-/-}$ double mutant mice (data not shown), which is in dramatic contrast to the devastation of the vasculature observed in both *npn-1* null mice and in mice lacking *npn-1* exclusively in endothelial cells. These findings support the idea that VEGF-Npn-1 signaling, but not Sema-Npn-1 signaling, is critical for general vasculature development. Finally, and surprisingly, both VEGF-Npn-1 and Sema-Npn-1 and/or -Npn-2 signaling coordinate septation of the cardiac outflow tract, while

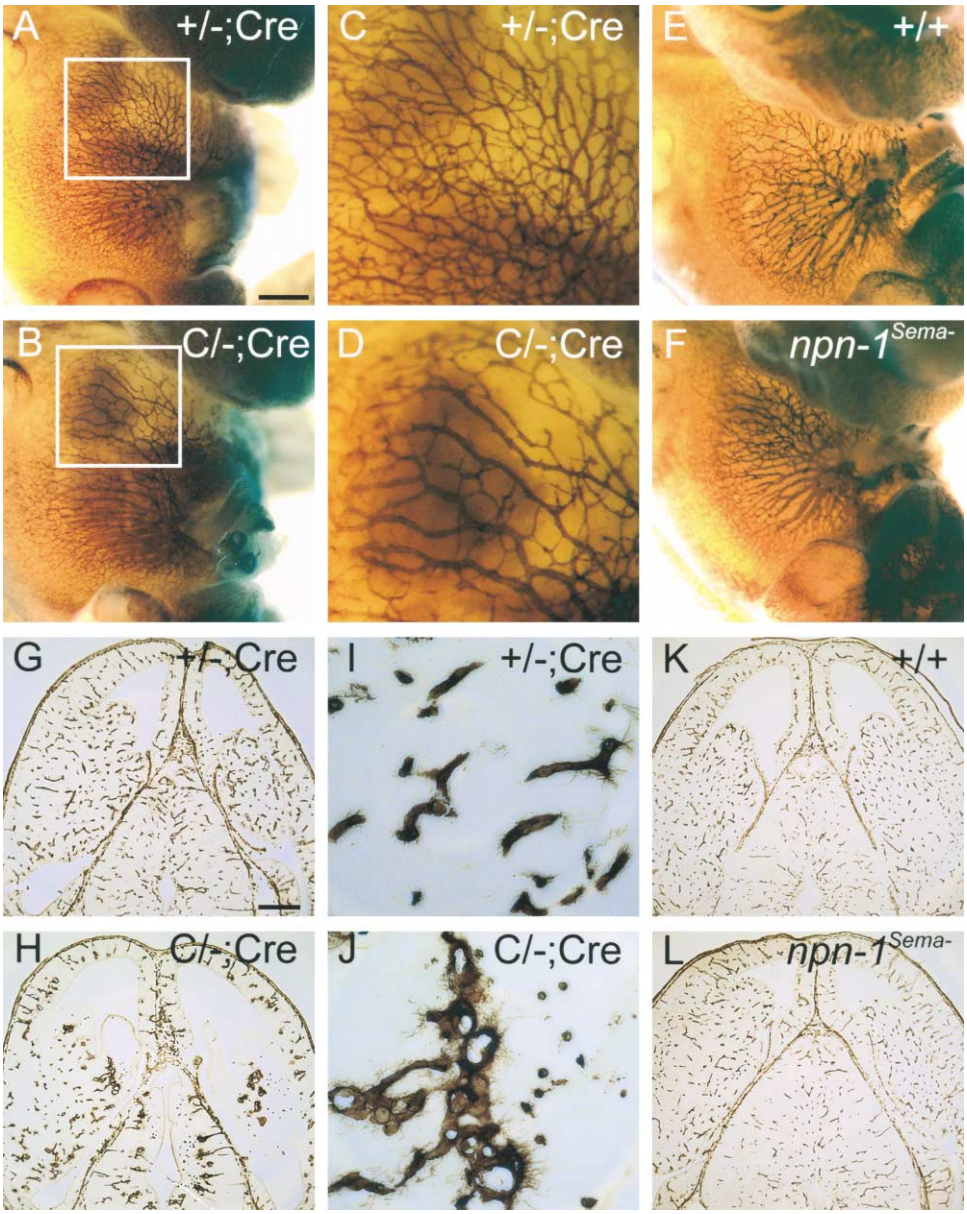

Figure 6. Severe Vasculature Disruption in Endothelial-Specific *npn-1* Null Mice, but Not in *npn-1*$^{Sema-}$ Mice

(A–F) Whole-mount anti-PECAM staining of a endothelial cell-specific *npn-1* null mutant (*C/−; Cre)* (B), a heterozygous littermate control (*+/−; Cre*) (A), homozygous *npn-1*$^{Sema-}$ (F), and a wild-type littermate control embryo (E), all at E12.5. Boxed regions from (A) and (B) are displayed at higher magnification in (C) and (D), respectively.

(G–L) Isolectin staining of E13.5 horizontal brain sections from a endothelial cell-specific *npn-1* null mutant embryo (*C/−; Cre)* (H), a heterozygous littermate control embryo (*+/−;Cre)* (G), a homozygous *npn-1*$^{Sema-}$ embryo (L), and a wild-type littermate control embryo (K). Select regions from (G) and (H) are displayed at higher magnification in (I) and (J), respectively. Note the decrease in endothelial branching in *C/−; Cre* mice compared to controls. Scale bars: (A, B, E, and F), 0.5 mm; (C and D), 0.2 mm; (G, H, K, and L), 350 μm; (I and J), 50 μm.

Sema3A-Npn-1 signaling in endothelial cells appears to control growth of the atria. Thus, Npn-1 is a versatile, multifunctional receptor for distinct families of ligands that coordinate heart, vasculature, and nervous system development.

Npn-1 and Nervous System Development

The chemorepellant Sema3A was the first identified ligand for Npn-1, and several lines of evidence indicate that Npn-1 is an obligate coreceptor for Sema3A, while Npn-2 is a coreceptor for Sema3F. Indeed, a comparison of the phenotypes of *Npn-1*$^{Sema-}$ mice and *sema3A* null mice indicates that these mutants partially phenocopy one another. For example, spinal and cranial nerves are defasciculated and abnormally extended in both mutant mice (Behar et al., 1996; Kitsukawa et al., 1997; Taniguchi et al., 1997). Moreover, entorhinal cortical axons are mistargeted in both *npn-1*$^{Sema-}$ mice and *sema3A* null mice (Pozas et al., 2001), although this phenotype is more dramatic in *npn-1*$^{Sema-}$ mice. This suggests that

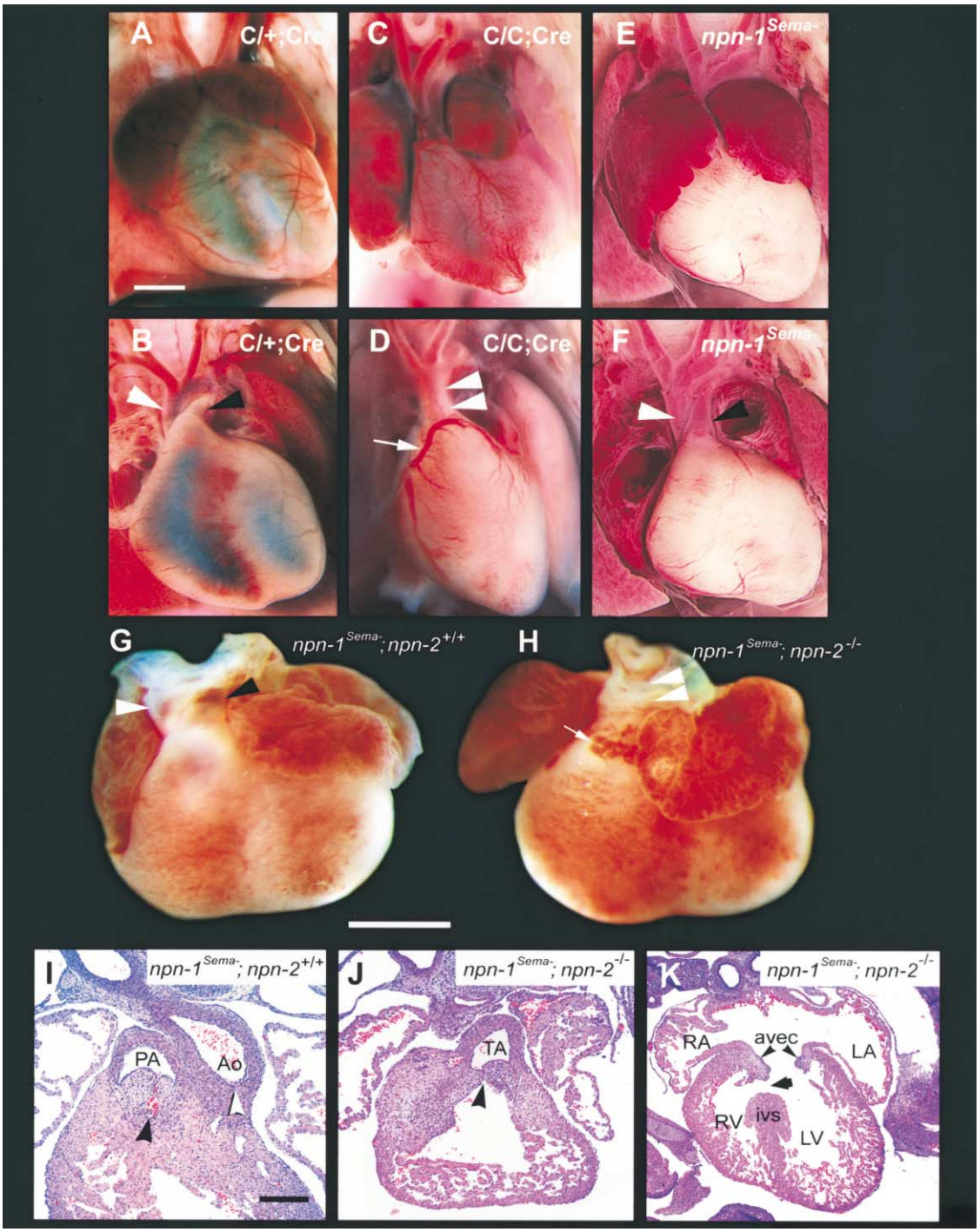

Figure 7. Cardiac Defects in Endothelial Cell-Specific *npn-1* Null Mice, *npn-1*$^{Sema-}$ Mice, and *npn-1*$^{Sema-}$;*npn-2*$^{-/-}$ Double Mutant Mice

(A–F) Gross examination of the hearts of wild-type (A and B), endothelial cell-specific *npn-1* null mice (*C/C;Cre*) (C and D), and *npn-1*$^{Sema-}$ mice (E and F). (A and B) Ventral view of a wild-type heart in which normal atria, ventricles, and vessels of the aortic arch can be seen (A). After removal of the anterior half of the atria (B), the right ventricular outflow tract can be clearly seen giving rise to the pulmonary trunk (black arrowhead). The aorta (white arrowhead) is distinctly visible arising posterior to the pulmonary trunk (B). The left anterior descending coronary artery (faint) courses normally through the interventricular sulcus. (C and D) Ventral view of the heart from a *C/C;Cre* mutant. There is marked right atrial enlargement (C). The ventricular outflow tract shows a common trunk (double arrowhead in [D]) giving rise to both the aorta and the pulmonary trunk (truncus arteriosus). Upon removal of the anterior half of the atria (D) an anomalous origin of the left coronary artery from the right side of the truncus arteriosus can be seen (white arrow), and this misplaced coronary artery crosses over the outflow tract to become the left anterior descending artery. (E and F) Ventral view of the heart of a *npn-1*$^{Sema-}$ mouse. There is bilateral atrial enlargement (E), but, upon removal of the atria, it is clear that the aorta, pulmonary arteries, and coronary arteries arise normally.

(G–K) Persistent truncus arteriosus in E14.5 *npn-1*$^{Sema-}$;*npn-2*$^{-/-}$ double mutant mice. (G and H) Gross examination of the heart. (G) Ventral view of a heart from an E14.5 *npn-1*$^{Sema-}$ mouse exhibiting a normal outflow tract. The aorta (white arrowhead) arises from its normal position

Table 1. Cardiac Defects in *C/C;Cre*, *npn-1^{Sema-}*, *npn-2$^{-/-}$*, and *npn-1^{Sema-};npn-2$^{-/-}$* Double Mutant Mice

Genotype	PTA	BAE	AOC	VSD
C/C;Cre	17/17	17/17	4/10	3/8
npn-1^{Sema-}	0/11	10/11	0/11	1/11
npn-2$^{-/-}$	0/8	0/4	0/4	0/4
npn-1^{Sema-};npn-2$^{-/-}$	6/9	8/9	3/9	2/6

Numbers show mice with defect/total mice examined. PTA, persistent truncus arteriosus; BAE, bilateral atrial enlargement; AOC, anomalous origin of the coronary arteries; VSD, ventricular septal defect.

Sema3A and one or more additional secreted semaphorins act through Npn-1 to instruct the layer-specific targeting of entorhinohippocampal projections. We have also observed several axon guidance defects in *npn-1^{Sema-}* mice that have not been reported in *sema3A* mutant mice. These include precocious entry of the TrkA-positive fibers into the spinal cord, defects in the formation of the corpus callosum, and aberrant projections of vestibular ganglion neurons within the inner ear. Sema3A, Sema3C, Sema3D, and Sema3E can each bind to Npn-1, and, therefore, these neuronal defects may be due to a lack of signaling by any or all of these four secreted semaphorins. Furthermore, while we have not observed defects in orientation of apical dendrites and axons of layer 5 cortical neurons in P2, P6, or P14 *npn-1^{Sema-}* mice, we have noted striking differences in both the length and complexity of their basal dendrites. Additional comparisons between *npn-1^{Sema-}* mice and mice lacking one or more genes encoding each of the class 3 semaphorins will be necessary to establish which of these ligands might instruct the fasciculation and targeting of axons and the growth of dendrites of Npn-1—expressing cortical neurons during development.

Npn-1 and Cardiovascular Development

To investigate Npn-1 function in vasculature development, we generated mice in which Npn-1 was specifically deleted in endothelial cells. We found that the vasculature is severely disrupted in *C/−;Cre* mice, indicating that Npn-1 is indeed required within endothelial cells for angiogenesis. These defects are likely due to a deficiency in VEGF-Npn-1 signaling since the vasculature of *npn-1^{Sema-}* mice appears normal.

Compared to the relatively simple cell-type- and ligand specificities of Npn-1 signaling requirements in the nervous system and vasculature, we found that heart development requires a remarkable degree of coordination between the families of ligands that signal through their common Npn-1 receptor. Taken together with previous reports, our observations support a model in which Npn-1 confers responsiveness of multiple cell types to both VEGF and semaphorin ligands and functions within endothelial cells to coordinate heart development. Our findings also indicate that VEGF-Npn-1 signaling in endothelial cells controls septation of the outflow tract and topographic origin of the coronary arteries. These results also support a model in which Sema3C signaling, through either Npn-1 or Npn-2, instructs outflow tract septation; however, the cell-type dependence of this signaling event is less clear. Indeed, Sema3C signaling is required for outflow tract development (Feiner et al., 2001), and this ligand can bind with high affinity to both Npn-1 and Npn-2. Interestingly, while a Npn-1/Npn-2 heterodimer was previously suggested to be a Sema3C receptor in sympathetic neurons (Chen et al., 1997, 1998; Takahashi et al., 1998), we observed outflow tract defects in the *npn-1^{Sema-}* mice only in a *npn-2* null background, strongly supporting a distinct model in which either Npn-1 or Npn-2 can serve as a Sema3C receptor in the developing heart. It has been suggested that Sema3C guides migrating cardiac neural crest cells as they take up residence in the proximal outflow tract, where they play a crucial role in outflow tract septation (Brown et al., 2001; Feiner et al., 2001). While our results are consistent with this possibility, they are also consistent with a Sema3C signaling requirement in another cell type, possibly endothelial cells, for outflow tract septation. In any case, our results indicate that a secreted semaphorin, Sema3C, and one or more members of the VEGF family of ligands signal through a common receptor, Npn-1, to coordinate septation of the cardiac outflow tract. Lastly, a Sema3A-Npn-1 signal is required for proper development of the atria, and this signal is likely propagated within endothelial cells since atrial enlargement was observed in *Sema3A* null mice (Behar et al., 1996) and in both the *C/C;Cre* mice and *npn-1^{Sema-}* mice reported here.

In summary, our findings show that members of distinct ligand families, semaphorins and VEGFs, act through a common receptor, Npn-1, to instruct axonal pathfinding in neurons and growth of the vasculature, respectively. Remarkably, through Npn-1, members of these same ligand families collaborate to orchestrate development of the heart. Thus, neuropilins have the unique capacity to mediate functional interactions between distinct families of ligands to coordinate complex morphogenic events during development.

Experimental Procedures

Generation of *npn-1^{Sema-}*, *npn-1* Conditional, and *npn-1* Null Mice

A bacterial artificial chromosome (BAC) containing *npn-1* exon 2 was obtained from Incyte genomics (Palo Alto, CA). A 9 kb BamHI/SalI fragment containing 1.4 kb of upstream intron sequence, exon

behind the pulmonary trunk. (H) Ventral view of the heart from a *npn-1^{Sema-};npn-2$^{-/-}$* double mutant mouse showing truncus arteriosus (white arrowheads) and an abnormal vascular proliferation (arrow) similar to that seen in (D) . (I–J) Hematoxylin and Eosin-stained paraffin sections (5 μM) through the heart of a E14.5 control littermate showing the right ventricular outflow tract and endocardial cushions forming the pulmonic valve (concave black arrowhead) (I). The endocardial cushions forming the aortic valve are caudal to this level of section but the root of the aorta is clearly formed (white arrowhead). The *npn-1^{Sema-};npn-2$^{-/-}$* double mutant embryos (J) showed a single common root to the aorta and pulmonary artery (truncus arteriosus; concave black arrowhead). Some double mutant embryos also showed ventricular septal defects (arrow) (K). RA, right atrium; LA, left atrium; RV, right ventricle; LV, left ventricle; ivs, interventricular septum; AVEC, atrioventricular endocardial cushions (black arrowheads). Scale bars: (A–F), 500 μm; (G and H), 1 mm; (I and J), 50 μm ; (K), 100 μm.

2, and 7 kb of downstream intron sequence was subcloned into pBluescript, and this plasmid served as a template for the construction of the targeting vectors. To generate the *npn-1*$^{Sema-}$ targeting vector, a *loxP*-flanked *neo* cassette was inserted into the SacI site, which is 333 bp upstream of exon2. Exon 2 was replaced with a mutated exon 2 encoding a 7 amino acid substitution (see Gu et al., 2002) using standard cloning techniques (Figure 1B). For generation of the conditional *npn-1* targeting vector, a *neo FRT/loxP* cassette (kindly provided by Kogo Takamiya and Richard Huganir, Johns Hopkins School of Medicine) was cloned into the SacI site of the BamHI/SalI fragment (Figure 1C). The targeting vectors were linearized with NotI, electroporated into 129.1 mouse strain embryonic stem (ES) cells, and ES cell clones were selected with G418 (300 μg/ml). ES cell clones were screened by PCR, and the results were confirmed by Southern blotting. Two conditional or four *npn-1*$^{Sema-}$ clones that successfully underwent homologous recombination were injected into C57Bl/6 blastocysts that were then introduced into pseudopregnant females. Chimeric animals were mated with C57Bl/6 to produce agouti heterozygous animals, and these mice were subsequently crossed with mice expressing either Cre recombinase (Schwenk et al., 1995) or FlpE recombinase (Rodriguez et al., 2000) in germ cells (kindly provided by Susan Dymecki, Harvard University) to excise the *neo* cassettes. *Npn-1* null mice were obtained by crossing conditional *npn-1* mice with mice expressing Cre recombinase in germ cells. Mice with the genotype *C/C; Cre* shown in Figures 7A–7D were produced by mating *C/C* mice with *C/+*; *Tie-2-Cre* mice. Offspring were genotyped by PCR using primers that detect both the Cre transgene and the *npn-1* conditional alleles. Mice with the genotype *C/−; Cre* (Figure 6) were produced by mating *C/−* mice (harboring one *C* allele and one *npn-1* null allele) with *C/+*; *Tie-2-Cre* mice. Offspring were genotyped by PCR using primers that detect the Cre allele, the *npn-1* conditional allele, and the *npn-1* null allele. Germline chimeras were crossed into a pure C57/Bl6 background, and all subsequent breeding was done in a C57/Bl6 background. All the analyses were performed on the F2–F5 generations.

AP Fusion Protein Binding to Tissue Sections

Fresh-frozen E12.5 and E17.5 embryos were sectioned using a cryostat, and AP fusion protein binding to tissue sections was performed as previously described (Giger et al., 1998).

DRG Repulsion Assay

DRG were dissected from E14.5 wild-type or mutant embryos, and collagen repulsion assays were performed essentially as previously described (Kolodkin et al., 1997). Statistical analysis was performed using a two-way ANOVA.

Whole-Mount Immunostaining and Immunohistochemical Procedures

Embryos were fixed in PBS containing 4% PFA, and whole-mount staining was performed as described (Giger et al., 2000) using primary monoclonal antibodies against either PECAM-1 (clone MEC13.3, isotype rat, 1:500 dilution; Pharmingen, San Diego, CA) or neurofilament 2H3 (supernatant from hybridoma cells; 1:50 dilution; Developmental Studies Hybridoma Bank, Iowa City, IA) and peroxidase-conjugated secondary antibodies. Immunocytochemistry of cryosections (20 μm) using rabbit anti-Npn-1 (Kolodkin et al., 1997), rabbit anti-TrkA antibody (1:1000; kindly provided by L. Reichardt, University of California, San Francisco), and 2H3 neurofilament antibody was performed as described (Giger et al., 2000).

DiI Labeling of Callosal and Entorhinohippocampal Projections

DiI labeling of callosal projections was performed on E17.5 embryos as described (Shu and Richards, 2001). 45 μm vibratome sections of DiI-labeled brains were immunostained with antibodies against glial fibrillary acidic protein (GFAP) as described (Shu and Richards, 2001). DiI labeling of entorhinohippocampal projections was performed on newborn mice (P0–P2) as described (Super et al., 1998; Super and Soriano, 1994).

Anterograde and Retrograde Labeling of Vestibulocochlear Projections

A fluorescent lipophilic tracer (PKH26) was used to label the peripheral and central projections of the vestibulocochlear nerve as previously described (Maklad and Fritzsch, 2002; Wilm and Fritzsch, 1993).

Visualization of Cortical Dendrites

The *thy1-GFP-m* mouse line was obtained from Joshua Sanes (Washington University School of Medicine) and *thy1-YFP -16Jrs* mice were obtained from Jackson Labs (Bar Harbor, MA). Both reporter lines were crossed with *npn-1*$^{Sema-/+}$ mice to obtain double heterozygous mice, which were then bred to obtain mutant mice (*npn-1*$^{Sema-}$*;thy1-GFP-m*, and *npn-1*$^{Sema-}$*;thy1-YFP*) and control littermates. P2, P6, and P14 mutant and littermate control mice were anesthetized and perfused with 4% paraformaldehyde. 100 μm (P14) and 40 μm (P2 and P6) coronal brain sections were made, mounted, and analyzed by confocal microscopy.

Acknowledgments

We thank members of the Kolodkin and Ginty laboratories, Jan Rosenbaum, Daniel Leahy, and Anirvan Ghosh for helpful discussions and comments on the manuscript. We thank Mitra Cowan and the Johns Hopkins Transgenic Facility for blastocyst injections and advice with ES cells, Guo Huang for help with the TrkA staining experiments, Sarah Lawson and Todd Hippe for excellent technical assistance, Naren Ramanan for help with preparation of the figures, Kogo Takamiya and Richard Huganir for advice with targeting vectors, Susan Dymecki for the germline FlpE mice, and Masashi Yanagisawa for the *Tie-2-Cre* mice. This work was supported by NIH/NRSA-5F32NS11016, NIH/NHLBI P01-HL70295, NIH/NIDCD R01-DC 005590, the Robert Packard Center for ALS Research at Johns Hopkins, NIH/NIMH-R01MH59199, the Kirsch Foundation, and the Howard Hughes Medical Institute.

Received: January 27, 2003
Revised: April 29, 2003
Accepted: May 7, 2003
Published: July 7, 2003

References

Behar, O., Golden, J.A., Mashimo, H., Schoen, F.J., and Fishman, M.C. (1996). Semaphorin III is needed for normal patterning and growth of nerves, bones, and heart. Nature *383*, 525–528.

Brown, C.B., Feiner, L., Lu, M.M., Li, J., Ma, X., Webber, A.L., Jia, L., Raper, J.A., and Epstein, J.A. (2001). PlexinA2 and semaphorin signaling during cardiac neural crest development. Development *128*, 3071–3080.

Chen, H., Chedotal, A., He, Z., Goodman, C.S., and Tessier-Lavigne, M. (1997). Neuropilin-2, a novel member of the neuropilin family, is a high affinity receptor for the semaphorins Sema E and Sema IV but not Sema III. Neuron *19*, 547–559.

Chen, H., He, Z., Bagri, A., and Tessier-Lavigne, M. (1998). Semaphorin-neuropilin interactions underlying sympathetic axon responses to class III semaphorins. Neuron *21*, 1283–1290.

Chen, H., Bagri, A., Zupicich, J.A., Zou, Y., Stoeckli, E., Pleasure, S.J., Lowenstein, D.H., Skarnes, W.C., Chedotal, A., and Tessier-Lavigne, M. (2000). Neuropilin-2 regulates the development of selective cranial and sensory nerves and hippocampal mossy fiber projections. Neuron *25*, 43–56.

Creazzo, T.L., Godt, R.E., Leatherbury, L., Conway, S.J., and Kirby, M.L. (1999). Role of cardiac neural crest cells in cardiovascular development. Annu. Rev. Physiol. *60*, 267–286.

Feiner, L., Webber, A.L., Brown, C.B., Lu, M.M., Jia, L., Feinstein, P., Mombaerts, P., Epstein, J.A., and Raper, J.A. (2001). Targeted disruption of semaphorin 3C leads to persistent truncus arteriosus and aortic arch interruption. Development *128*, 3061–3070.

Feng, G., Mellor, R.H., Bernstein, M., Keller-Peck, C., Nguyen, Q.T., Wallace, M., Nerbonne, J.M., Lichtman, J.W., and Sanes, J.R. (2000).

Imaging neuronal subsets in transgenic mice expressing multiple spectral variants of GFP. Neuron *28*, 41–51.

Ferrara, N. (2001). Role of vascular endothelial growth factor in regulation of physiological angiogenesis. Am. J. Physiol. Cell Physiol. *280*, C1358–C1366.

Fujisawa, H., Kitsukawa, T., Kawakami, A., Takagi, S., Shimizu, M., and Hirata, T. (1997). Roles of a neuronal cell-surface molecule, neuropilin, in nerve fiber fasciculation and guidance. Cell Tissue Res. *290*, 465–470.

Giger, R.J., Urquhart, E.R., Gillespie, S.K.H., Levengood, D.V., Ginty, D.D., and Kolodkin, A.L. (1998). Neuropilin-2 is a receptor for semaphorin IV: insight into the structural basis of receptor function and specificity. Neuron *21*, 1079–1092.

Giger, R.J., Cloutier, J.F., Sahay, A., Prinjha, R.K., Levengood, D.V., Moore, S.E., Pickering, S., Simmons, D., Rastan, S., Walsh, F.S., et al. (2000). Neuropilin-2 is required in vivo for selective axon guidance responses to secreted semaphorins. Neuron *25*, 29–41.

Gu, C., Limberg, B.J., Whitaker, G.B., Perman, B., Leahy, D.J., Rosenbaum, J.S., Ginty, D.D., and Kolodkin, A.L. (2002). Characterization of neuropilin-1 structural features that confer binding to semaphorin 3A and vascular endothelial growth factor *165*. J. Biol. Chem. *277*, 18069–18076.

He, S., and Tessier-Lavigne, M. (1997). Molecular basis of axonal chemorepulsion: neuropilin is a semaphorin/collapsin receptor. Cell *90*, 739–751.

He, Z., Wang, K.C., Koprivica, V., Ming, G., and Song, H.J. (2002). Knowing how to navigate: mechanisms of semaphorin signaling in the nervous system, Sci STKE *2002*, RE1.

Huber, A.B., Kolodkin, A.L., Ginty, D.D., and Cloutier, J.F. (2003). Signaling at the growth cone: ligand-receptor complexes and the control of axon growth and guidance. Annu. Rev. Neurosci., in press. Published online June 16, 2003. 10.1146/annurev.neuro.26.010302.081139.

Kawasaki, T., Kitsukawa, T., Bekku, Y., Matsuda, Y., Sanbo, M., Yagi, T., and Fujisawa, H. (1999). A requirement for neuropilin-1 in embryonic vessel formation. Development *126*, 4895–4902.

Kisanuki, Y.Y., Hammer, R.E., Miyazaki, J., Williams, S.C., Richardson, J.A., and Yanagisawa, M. (2001). Tie2-Cre transgenic mice: a new model for endothelial cell-lineage analysis in vivo. Dev. Biol. *230*, 230–242.

Kitsukawa, T., Shimizu, M., Sanbo, M., Hirata, T., Taniguchi, M., Bekku, Y., Yagi, T., and Fujisawa, H. (1997). Neuropilin-semaphorin III/D-mediated chemorepulsive signals play a crucial role in peripheral nerve projection in mice. Neuron *19*, 995–1005.

Kolodkin, A.L., Levengood, D.V., Rowe, E.G., Tai, U.-T., Giger, R.J., and Ginty, D.D. (1997). Neuropilin is a semaphorin III receptor. Cell *90*, 753–762.

Lee, P., Goishi, K., Davidson, A.J., Mannix, R., Zon, L., and Klagsbrun, M. (2002). Neuropilin-1 is required for vascular development and is a mediator of VEGF-dependent angiogenesis in zebrafish. Proc. Natl. Acad. Sci. USA *99*, 10470–10475.

Maklad, A., and Fritzsch, B. (2002). The developmental segregation of posterior crista and saccular vestibular fibers in mice: a carbocyanine tracer study using confocal microscopy. Brain Res. Dev. Brain Res. *135*, 1–17.

Neufeld, G., Cohen, T., Gengrinovitch, S., and Poltorak, Z. (1999). Vascular endothelial growth factor (VEGF) and its receptors. FASEB J. *13*, 9–22.

Neufeld, G., Cohen, T., Shraga, N., Lange, T., Kessler, O., and Herzog, Y. (2002). The neuropilins: multifunctional semaphorin and VEGF receptors that modulate axon guidance and angiogenesis. Trends Cardiovasc. Med. *12*, 13–19.

Oosthuyse, B., Moons, L., Storkebaum, E., Beck, H., Nuyens, D., Brusselmans, K., Van Dorpe, J., Hellings, P., Gorselink, M., Heymans, S., et al. (2001). Deletion of the hypoxia-response element in the vascular endothelial growth factor promoter causes motor neuron degeneration. Nat. Genet. *28*, 131–138.

Polleux, F., Giger, R.J., Ginty, D.D., Kolodkin, A.L., and Ghosh, A. (1998). Patterning of cortical efferent projections by semaphorin-neuropilin interactions. Science *282*, 1904–1906.

Polleux, F., Morrow, T., and Ghosh, A. (2000). Semaphorin 3A is a chemoattractant for cortical apical dendrites. Nature *404*, 567–573.

Pozas, E., Pascual, M., Nguyen Ba-Charvet, K.T., Guijarro, P., Sotelo, C., Chedotal, A., Del Rio, J.A., and Soriano, E. (2001). Age-dependent effects of secreted Semaphorins 3A, 3F, and 3E on developing hippocampal axons: in vitro effects and phenotype of Semaphorin 3A (−/−) mice. Mol. Cell. Neurosci. *18*, 26–43.

Rodriguez, C.I., Buchholz, F., Galloway, J., Sequerra, R., Kasper, J., Ayala, R., Stewart, A.F., and Dymecki, S.M. (2000). High-efficiency deleter mice show that FLPe is an alternative to Cre-loxP. Nat. Genet. *25*, 139–140.

Romero, A., Romao, M.J., Varela, P.F., Kolln, I., Dias, J.M., Carvalho, A.L., Sanz, L., Topfer-Petersen, E., and Calvete, J.J. (1997). The crystal structures of two spermadhesins reveal the CUB domain fold. Nat. Struct. Biol. *4*, 783–788.

Schwenk, F., Baron, U., and Rajewsky, K. (1995). A cre-transgenic mouse strain for the ubiquitous deletion of loxP-flanked gene segments including deletion in germ cells. Nucleic Acids Res. *23*, 5080–5081.

Shimizu, M., Murakami, Y., Suto, F., and Fujisawa, H. (2000). Determination of cell adhesion sites of neuropilin-1. J. Cell Biol. *148*, 1283–1293.

Shu, T., and Richards, L.J. (2001). Cortical axon guidance by the glial wedge during the development of the corpus callosum. J. Neurosci. *21*, 2749–2758.

Soker, S., Takashima, S., Miao, H.-Q., Neufeld, G., and Klagsbrun, M. (1998). Neuropilin-1 is expressed by endothelial and tumor cells as an isoform-specific receptor for vascular endothelial growth factor. Cell *92*, 735–745.

Sondell, M., Lundborg, G., and Kanje, M. (1999). Vascular endothelial growth factor has neurotrophic activity and stimulates axonal outgrowth, enhancing cell survival and Schwann cell proliferation in the peripheral nervous system, J. Neurosci. *19*, 5731–5740.

Sondell, M., Sundler, F., and Kanje, M. (2000). Vascular endothelial growth factor is a neurotrophic factor which stimulates axonal outgrowth through the flk-1 receptor. Eur. J. Neurosci. *12*, 4243–4254.

Super, H., and Soriano, E. (1994). The organization of the embryonic and early postnatal murine hippocampus. II. Development of entorhinal, commissural, and septal connections studied with the lipophilic tracer DiI. J. Comp. Neurol. *344*, 101–120.

Super, H., Martinez, A., Del Rio, J.A., and Soriano, E. (1998). Involvement of distinct pioneer neurons in the formation of layer-specific connectins in the hippocampus. J. Neurosci. *18*, 4616–4626.

Takagi, S., Tsuji, T., Amagai, T., Takamatsu, T., and Fujisawa, H. (1987). Specific cell surface labels in the visual center of *Xenopus laevis* tadpole identified using monoclonal antibodies. Dev. Biol. *122*, 90–100.

Takahashi, T., Nakamura, F., Jin, Z., Kalb, R., and Strittmatter, S. (1998). Semaphorins A and E act as antagonists of neuropilin-1 and agonists of neuropilin-2 receptors. Nat. Neurosci. *1*, 487–493.

Takashima, S., Kitakaze, M., Asakura, M., Asanuma, H., Sanada, S., Tashiro, F., Niwa, H., Miyazaki Ji, J., Hirota, S., Kitamura, Y., et al. (2002). Targeting of both mouse neuropilin-1 and neuropilin-2 genes severely impairs developmental yolk sac and embryonic angiogenesis. Proc. Natl. Acad. Sci. USA *99*, 3657–3662.

Taniguchi, M., Yuasa, S., Fujisawa, H., Naruse, I., Saga, S., Mishina, M., and Yagi, T. (1997). Disruption of semaphorin *III/D* gene causes severe abnormality in peripheral nerve projection. Neuron *19*, 519–530.

Wilm, C., and Fritzsch, B. (1993). Regenerating retinal fibers display error-free homing along undamaged normal fibers. J. Neurobiol. *24*, 898–902.

Yuan, L., Moyon, D., Pardanaud, L., Breant, C., Karkkainen, M.J., Alitalo, K., and Eichmann, A. (2002). Abnormal lymphatic vessel development in neuropilin 2 mutant mice. Development *129*, 4797–4806.